

1-MW BEAM OPERATION SCENARIO IN THE J-PARC RCS

H. Hotchi[#], H. Harada, N. Hayashi, M. Kinsho, P.K. Saha, Y. Shobuda, F. Tamura, K. Yamamoto, M. Yamamoto, and M. Yoshimoto, J-PARC, JAEA, Tokai, Ibaraki, 319-1195, Japan
Y. Irie, KEK, Tsukuba, Ibaraki, 305-0801, Japan

Abstract

The injection energy of the J-PARC RCS will be upgraded from 181 MeV to 400 MeV in the 2013 summer-autumn period. With this upgraded injection energy, we are to aim at the 1 MW design output beam power. In this paper, we discuss beam dynamics issues for the 1 MW beam operation and their possible solutions.

INTRODUCTION

The 3-GeV Rapid Cycling Synchrotron (RCS) of the J-PARC has two functions as a proton driver to produce pulsed muons and neutrons at the Materials and Life Science Experimental Facility (MLF) and as an injector to the following 50-GeV Main Ring Synchrotron (MR), aiming at 1 MW output beam power which is the highest level in the world.

As shown in Fig. 1, a H^- beam from the linac is delivered to the RCS injection point, where it is multi-turn charge-exchange injected through a carbon stripper foil. The RCS accelerates the injected protons up to 3 GeV with a repetition rate of 25 Hz. Most of the time, the 3 GeV beam from the RCS is transported to the MLF, while only a portion of the RCS beam (typically four pulses every several seconds) is transported to the MR, where the beam destination is switched pulse-by-pulse by employing a pulse dipole magnet installed downstream of the RCS extraction section.

The current injection energy is 181 MeV. With this injection energy, the RCS first aims at providing more than 300 kW output beam power. The linac will be upgraded in the 2013 summer-autumn period; the output energy will be improved to 400 MeV with the addition of an annular coupled structure (ACS) linac, and the maximum peak current will be increased from 30 to 50 mA by replacing the front-end system (ion source and rf quadrupole linac). After that, we are to aim at our final goal of the 1 MW design output beam power.

The J-PARC beam commissioning began in November 2006 from the linac to the downstream facilities. The RCS was beam commissioned in October 2007. Following the initial beam tuning [1], the RCS was made available for user operation in December 2008 with an output beam power of 4 kW. Since then, the RCS beam power ramp-up has proceeded well. The major beam loss issues observed in high-intensity beam trials of up to 420 kW have been solved so far [2]. In this process, the output beam power for the routine user program has been increased to 280 kW to date.

Thus, now the RCS is in transition from the initial commissioning phase to the final stage aiming at the 1

MW output beam power. Our efforts hereafter will be focused on establishing the 1 MW design beam operation.

In this paper, we discuss beam dynamics issues for the 1 MW beam operation and their solutions aiming for beam loss reduction, better operational flexibility, and high-quality (low-halo/tail) output beam, on the basis of numerical simulations with a 3-dimensional particle tracking code “Simpsons”. As described in [2], this numerical simulation well reproduces beam loss patterns and behaviors of transverse and longitudinal beam profiles measured so far. The same manner was applied to the present 1 MW beam simulation with the injection energy of 400 MeV.

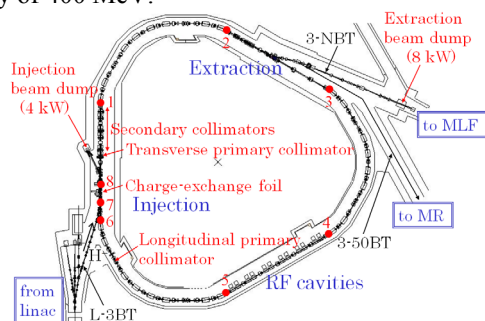


Figure 1: Schematic of the RCS.

BEAM LOSS EXPECTED FOR 1 MW BEAM OPERATION

The most important issues in increasing the output beam power are the control and minimization of beam loss to keep machine activation within the permissible level. There are many sources of beam loss, in which the most critical one is the space charge effect in the low energy region. It generally imposes a major performance limit on high-power proton synchrotrons. To alleviate this, the RCS adopts transverse and longitudinal injection painting technique.

The major beam loss issues observed in high-intensity beam experiments of up to 420 kW with the injection energy of 181 MeV have already been solved; the large beam loss of 18% observed at the injection energy region for a 420 kW intensity beam was well reduced to less than 1% by transverse and longitudinal injection painting [2]. In the transverse painting, here, 100π -mm-mrad (ϵ_{tp}) correlated painting was employed. On the other hand, in the longitudinal painting [3,4], the momentum offset injection of -0.2% ($\Delta p/p$) was applied in combination with superposing the second harmonic rf with an amplitude of 80% (V_2/V_1) of the fundamental one. As an additional control in the longitudinal painting, the linear phase sweep from -100 to 0 degrees (ϕ_2) of the second

[#]hotchi.hideaki@jaea.go.jp

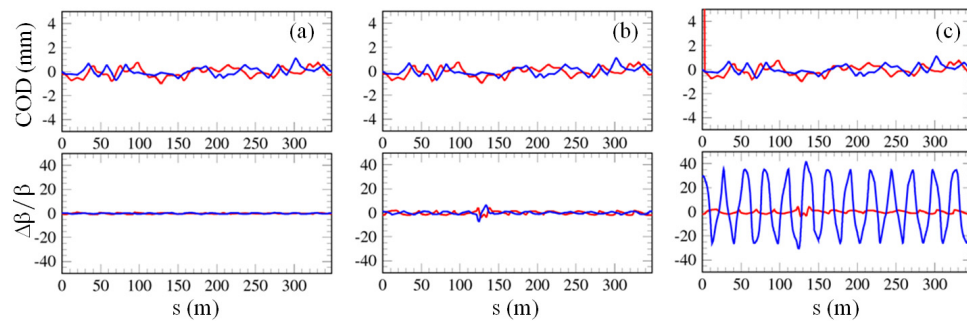


Figure 2: Distortion of the optical function caused by lattice imperfections, where the red curves shows the horizontal ones and the blue curves are for the vertical ones; (a) shows the distortion calculated with only the field and alignment errors, (b) adds the leakage field, and (c) adds the edge focus.

harmonic rf was also applied during injection, which enables further bunch distribution control through a dynamical change of the rf bucket potential. The remaining beam loss for the 420 kW intensity beam arises mainly from foil scattering during charge exchange injection. This means the beam loss in the RCS has been well minimized for beam intensities of up to 420 kW.

The space charge effect at 400 MeV for the 1 MW intensity beam is almost equivalent to that at 181 MeV for the 420 kW intensity beam. As is shown in Fig.3 given later, the beam loss in the 1 MW numerical beam simulation was well minimized with the similar injection painting parameter to that optimized in the above beam experiment, as expected. The residual beam loss was evaluated to be 0.3%, which is from foil scattering during injection. The corresponding beam loss power is 400 W, which is much less than the ring collimator limit of 4 kW.

EFFORT FOR EXPANDING TRANSVERSE PAINTING AREA

One of the remaining issues in the RCS beam operation is that the variable range of transverse painting emittance is limited to 100π mm mrad by lattice imperfections, which is almost half of the design value of 216π mm mrad. As already mentioned, the beam loss in the RCS can be well minimized for beam intensities of up to 1 MW by the combination of the full longitudinal painting and the limited transverse painting of 100π mm mrad, but this situation leaves a strong limit for the operational flexibility, in particular, for tune-ability, because of the large residual space-charge tune shift of around -0.4 .

In this section, we discuss possible schemes for getting sufficient variable range of transverse painting and better operational flexibility for the 1-MW beam operation. In the present work, the operating point was set at (6.43, 6.43). This operating point allows the space-charge tune shift to avoid serious multipole resonances.

Lattice Imperfections and Their Contributions to Beam Loss

In the RCS, there are two kinds of lattice imperfections, except for basic random field and alignment errors. One is a static leakage field from the extraction beam line dc magnets. This leakage field includes a quadrupole field

component as well as a simple dipole kick component.

The issue caused by the leakage field is that its quadrupole field component affects the beam motion through a distortion of the accelerator super-periodicity. Another lattice imperfection is found in the injection section. In the RCS, beam injection is performed with a horizontal local bump orbit formed by four sets of rectangular pulse dipole magnets. This four-bump method generates edge focus at the entrance and exit of the injection bump magnets, causing beta function beating especially on the vertical plane during injection. Details of beam-based estimations of such imperfection fields are described in [5].

Figure 2 shows a distortion of the optical function caused by the lattice imperfections. The beta function beating caused by the field and alignment errors is only 1% (a), but it deteriorates into 7% (b) and 35% (c) with the addition of the leakage field and the edge focus. The state of the lattice property gradually changes from (c) to (a) as the acceleration progresses. Plot (c) corresponds to the optical function when the injection bump is active for injection, while plot (b) represents the situation when the injection bump is inactive just after injection. Then plot (b) gradually changes to (a) as the acceleration progresses, because the effect of the static leakage field gradually fades out with the acceleration. We investigated the effects of these lattice imperfections on the beam loss and their possible correction schemes.

Figure 3 shows a transverse painting area dependence of beam loss calculated with the systematic combinations of the lattice imperfections. In this calculation, the full longitudinal painting is also included with the transverse painting. In this figure the black line shows the result obtained with no lattice imperfection. In this case the beam loss can be kept at sufficiently low level of less than 1% over the whole range of transverse painting area up to 216π mm mrad. But the lattice imperfections push up the beam loss especially for large transverse painting. In this figure, the beam loss increase from black to red corresponds to the contribution from the basic random field and alignment errors. Since this part of beam loss arises mainly from a decrease of the collimator aperture caused by residual COD shown in Fig. 2 (a), it can be decreased simply by adjusting the centroid of the collimator gap following the COD. The main issue in the

present work is the beam loss increases from red to green and from green to blue caused by the edge focus and the leakage field. These lattice imperfections include focusing field errors. They excite various random resonances through a distortion of the super-periodicity, causing shrinkage of the dynamic aperture. This is main reason of the beam loss for the large transverse painting caused by the edge focus and the leakage field.

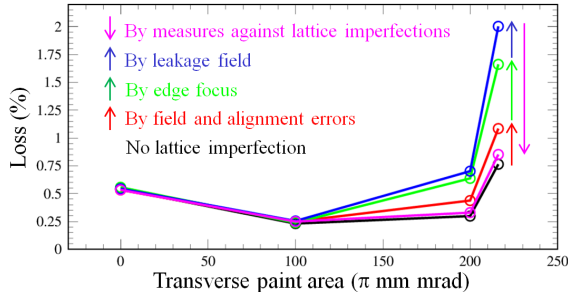


Figure 3: Transverse painting area dependence of beam loss calculated with the systematic combinations of the lattice imperfections.

Possible Measures Against Beam Loss Appearing for Large Transverse Painting

The measure against the leakage field is straightforward, namely it is simply to add magnetic shields. We will aim at decreasing the leakage field by an order of magnitude from the current value by reinforcing magnetic shields before the start-up of the 400 MeV injection. If realizing this, the corresponding beam loss disappears.

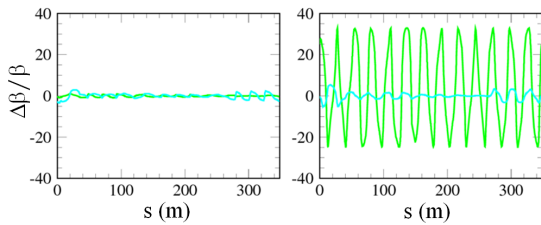


Figure 4: horizontal (left) and vertical (right) beta function beating during injection calculated without (green) and with (light blue) the quadrupole correctors.

The measure against the edge focus is also clear, namely it is to compensate the beta function beating caused by the edge focus during injection. For this purpose, we plan to install several sets of quadrupole correctors before the start-up of the 400 MeV injection. The locations proposed for them are shown by red circles in Fig. 1; six sets at both ends of each long straight insertion (1-6), and two sets at both ends of injection bump magnets (7-8) if necessary. As shown in Fig. 4, the large beta function beating of 35% on the vertical plane can be corrected to less than 5% by using the quadrupole correctors.

The hardware design of the quadrupole correctors is in progress at present. Figure 5 shows the calculated field distribution of the quadrupole corrector. The higher order field components intrinsic in the quadrupole corrector

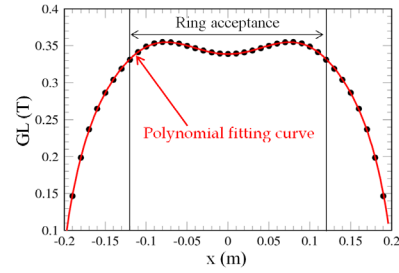


Figure 5: Calculated field distribution of the quadrupole corrector.

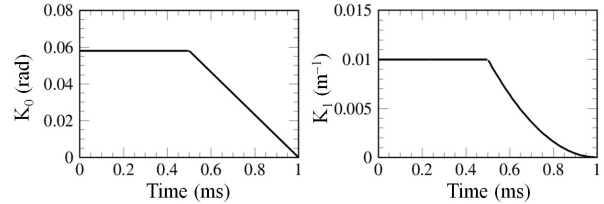


Figure 6: Time response of the injection bump magnet (left) and the quadrupole corrector (right).

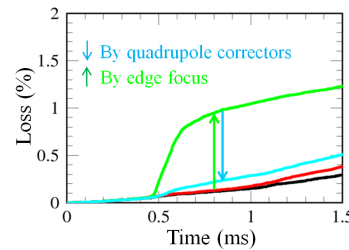


Figure 7: Time dependence of beam loss for the first 1.5 ms calculated for the large painting of 216π mm mrad without (green) and with (light blue) the quadrupole correctors.

were evaluated by fitting this field distribution with a polynomial function. As shown in the left plot in Fig. 6, the field pattern of the injection bump magnets consists of two parts, 0.5 ms flat-top for beam injection and 0.5 ms linear falling part. The strength of the edge focus is proportional to the square of the kick angle of the injection bump magnet. Therefore, for the falling part of the field pattern of the quadrupole corrector, the quadratic like time response is required as shown in the right plot in Fig. 6. We investigated the effectiveness of this correction scheme by numerical simulation including the realistic field distribution and time response of the quadrupole correctors. Fig. 7 shows the time dependence of beam loss for the first 1.5 ms calculated with the large painting of 216π mm mrad. In this figure, the difference from red to green corresponds to the beam loss increase caused by the edge focus, while that from green to light blue shows the beam loss decrease achieved by the quadrupole correctors; the quadrupole correctors well decreases the beam loss arising from the edge focus through the restoration of the lattice periodicity.

The rose line in Fig. 3 shows the beam loss calculated with all the above measures. Most of the beam loss

caused by the lattice imperfections is well suppressed with those measures. In this case, the beam loss can be kept at less than 1% over the whole range of transverse painting. This leads to better operational flexibility for the 1 MW beam operation, such as the flexible control of the space-charge tune shift as shown in Fig. 8, large tune shift with small painting and small tune shift with large painting. Also this will lead to better tune-ability for the 1-MW beam operation.

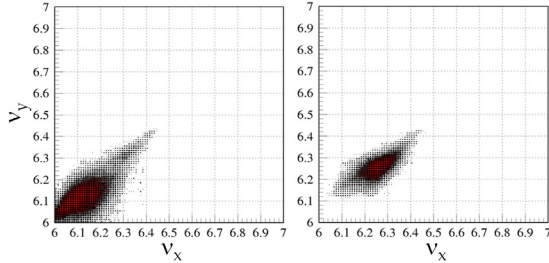


Figure 8: Space charge tune shift at the end of injection calculated for the transverse painting of 100π (left) and 216π (right) mm mrad.

EFFORT FOR REALIZING LOW-HALO/TAIL OUTPUT BEAM

Another issue for the 1 MW beam operation is to improve the quality of the extraction beam, namely to realize low-halo/tail beams. This is essential particularly for beam injection to the MR, since the MR has a relatively small physical aperture (81π mm mrad) compared to that of the beam line to the MLF (324π mm mrad). For the MR, the 3GeV beam from the RCS is transported via the 3-50BT to the injection point, as shown in Fig. 1. In the 3-50BT, a collimation system is installed. The aperture of the 3-50BT collimator is typically set at 54π mm mrad, where a tail component of the RCS beam is removed. Therefore, the first matter for the MR injection is to pass the beam through the 3-50BT collimator within the permissible beam loss level.

Emittance Growth in The Low Energy Region and Its Mitigation Scheme

As shown in Fig. 3, the beam loss for the 1 MW beam operation is minimized by the combination of the 100π -mm-mrad correlated transverse painting and the full longitudinal painting.

The left plot in Fig. 9 shows the time evolution of transverse normalized emittance (99%) for the first 6 ms calculated with the above injection painting parameter. In this figure, one can see remarkable emittance growth after 1 ms. Though this emittance growth hardly contributes to the beam loss in the RCS, it makes a major part of the beam loss at the 3-50BT collimator. The right plot in Fig. 9 shows the corresponding calculated time dependence of the bunching factor. By comparing these plots, one can find the emittance growth proceeds following the decrease of the bunching factor after 1 ms. If the bunching factor decreases in this low energy region, a

part of the beam particles reaches to the integer lines of $v_{x,y} = 6$ (see the left plot in Fig. 8 for reference). On these integer lines, there exist all-order systematic resonances, by which the beam particles suffer from the emittance dilution. If this consideration is correct, the emittance growth can be suppressed by minimizing the effects from the integer lines through further charge density control after 1 ms as well as during injection.

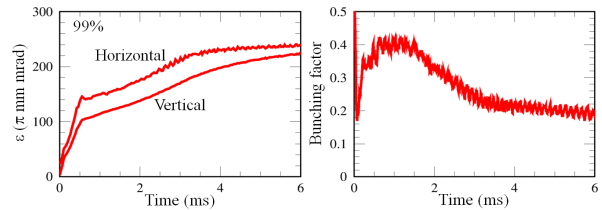


Figure 9: Left; Normalized transverse emittance (99%) calculated for the first 6 ms with the original injection painting parameter (ID 2 in Table 1 given later). Right; Corresponding bunching factor.

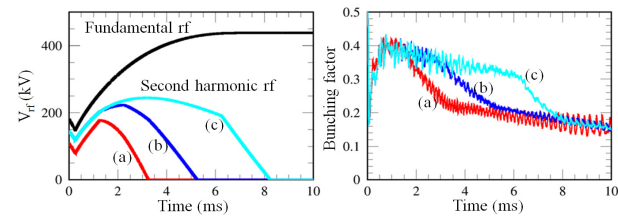


Figure 10: Left; Second harmonic rf with different durations (3-8 ms) applied for longitudinal painting in the present work. Right; Corresponding bunching factors.

Table 1: Injection Painting Parameters

ID	ϵ_{tp} (π mm mrad)	V_2/V_1 (%)	ϕ_2 (deg)	$\Delta p/p$ (%)
1	—	80 (a) in Fig.10	-100 to 0	-0.2
2	100	80 (a) in Fig.10	-100 to 0	-0.2
3	—	80 (b) in Fig.10	-100 to 0	-0.2
4	100	80 (b) in Fig.10	-100 to 0	-0.2
5	—	80 (c) in Fig.10	-100 to 0	-0.2
6	100	80 (c) in Fig.10	-100 to 0	-0.2

The left plot in Fig. 10 shows second harmonic rf voltage patterns used for longitudinal painting in the present work [6]. They have different durations (3–8 ms), in which the shortest pattern corresponds to the original one. As shown in the right plot in Fig. 10, longitudinal painting with the longer second harmonic rf duration acts to maintain large bunching factor over the first several ms. In this work, the behavior of the emittance growth in the low energy region and its contribution to the extraction beam halo were systematically investigated for longitudinal painting with the different second harmonic rf durations in Fig. 10 and their combinations with transverse painting. Injection painting parameters tested in the present work are summarized in Table 1.

Figure 11 shows the time evolution of transverse normalized emittance (99%) calculated for the first 6 ms with the painting parameter IDs in Table 1. As shown in this figure, longitudinal painting with the longer second

harmonic rf duration significantly mitigates the emittance growth, as expected. The longer second harmonic rf also assists the effect of transverse painting on the emittance growth mitigation. Transverse painting well suppresses the emittance growth during charge accumulation, but this effect vanishes following the decrease of bunching factor after 1 ms, as shown by the data ID 2 in Fig. 11, because of the influence from the integer lines. The longer second harmonic rf improves this situation, as shown by the data ID 6 in Fig. 11.

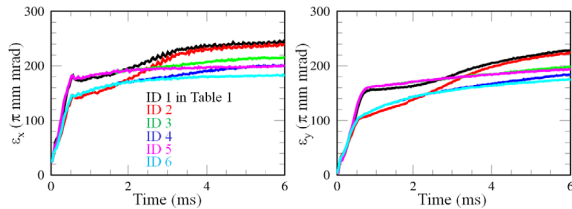


Figure 11: Horizontal (left) and vertical (right) normalized emittance (99%) calculated for the first 6 ms with the painting parameter IDs in Table 1.

Recently the effectiveness of this scheme for the emittance growth mitigation in the low energy region has been experimentally confirmed for a 420 kW intensity beam. By the combination of longitudinal painting with long-duration second harmonic rf and transverse painting, the beam loss at the 3-50BT collimator was successfully decreased to less than half of the original value [7].

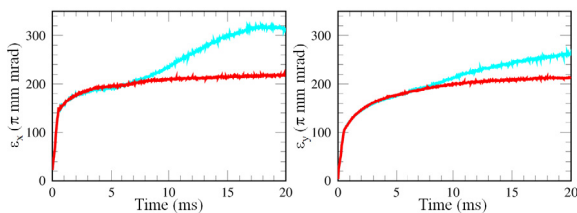


Figure 12: Horizontal (left) and vertical (right) normalized emittance (99%) for the whole period of 20 ms calculated without (light blue) and with (red) the tune manipulation (given in Fig. 13 later) for the painting parameter ID 6 in Table 1.

Emittance Growth in The Middle Stage of Acceleration Process and Its Mitigation Scheme

The light blue curve in Fig. 12 shows the time evolution of transverse normalized emittance calculated for the whole period of 20 ms with the painting parameter ID 6 in Table 1. In this curve, we can clearly see remarkable beam halo formation after 6 ms. A possible cause of this emittance growth is resonance cross for the acceleration process. If this consideration is correct, this emittance growth can be suppressed by dynamical tune control. Fig. 13 shows tune footprints calculated at 1.6~12.4 ms after the beginning of injection, in which the green arrows show the variation of the lattice tune controlled with 7 families of main quadrupole field patterns. Such a dynamic tune control is feasible by the current main quadrupole system. As shown in this figure,

this tune variation prevents beam particles from crossing the 3rd- and 4th-order random resonances which can be excited through a distortion of the super-periodicity caused by the lattice imperfections. As shown by the red curve in Fig. 12, the emittance growth observed at the middle stage of acceleration process is well suppressed by this tune manipulation.

Beam Halo/Tail Reduction Achieved by Improved Injection Painting and Tune Manipulation

By the combination of the improved injection painting (ID 6 in Table. 1) and the dynamical tune control (Fig. 13), the beam loss at the 3-50BT collimator was drastically decreased from 9.0 to 1.8%. If assuming the MR design output beam power of 0.75 MW (4-pulse injection to the MR every 2.12 seconds), this beam loss of 1.8% corresponds to 1.3 kW in power. Thanks to the above schemes, the beam loss at the 3-50BT collimator for the 1 MW intensity beam from the RCS is well suppressed within the current 3-50BT collimator capability of 2 kW.

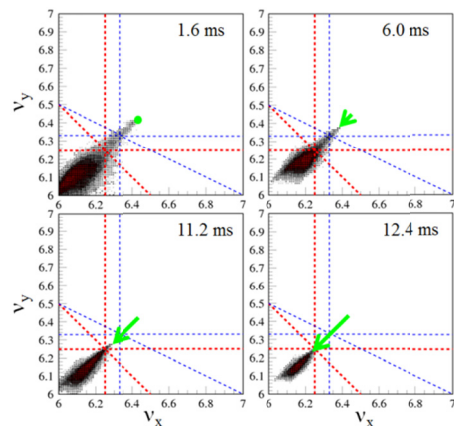


Figure 13: Tune footprints calculated at 1.6~12.4 ms after the beginning of injection, in which the green arrows show the variation of the lattice tune controlled with 7 families of main quadrupole field patterns.

FUTURE PLAN

The parameter optimization work will continue aiming for higher-quality higher-power beams that meet the requirements of the downstream facilities.

The RCS will start beam tuning with the upgraded linac in January 2014, aiming at our final goal of the 1 MW output beam power.

REFERENCES

- [1] H. Hotchi et al., PRST-AB **12**, 040402 (2009).
- [2] H. Hotchi et al., PRST-AB **15**, 040402 (2012).
- [3] F. Tamura et al., PRST-AB **12**, 041001 (2009).
- [4] M. Yamamoto et al., NIM, A **621**, 15 (2010).
- [5] H. Hotchi et al., Proceedings of IPAC'11, p.6.
- [6] M. Yamamoto, private communication.
- [7] H. Hotchi et al., Proceedings of IPAC'12, p.3918.